Sustainable Cities and Society 96 (2023) 104712

Contents lists available at ScienceDirect

Sustainable Cities and Society

journal homepage: www.elsevier.com/locate/scs

Crowding on public transport using smart card data during the COVID-19 pandemic: New methodology and case study in Chile☆

Franco Basso [a,b,*], Jonathan Frez [c], Hugo Hernández [a], Víctor Leiva [a], Raúl Pezoa [d], Mauricio Varas [e]

[a] Escuela de Ingeniería Industrial, Pontificia Universidad Católica de Valparaíso, Valparaíso, Chile
[b] Instituto Sistemas Complejos de Ingeniería (ISCI), Chile
[c] Escuela de Ingeniería Informática y Telecomunicaciones, Universidad Diego Portales, Santiago, Chile
[d] Escuela de Ingeniería Industrial, Universidad Diego Portales, Santiago, Chile
[e] Centro de Investigación en Sustentabilidad y Gestión Estratégica de Recursos, Universidad del Desarrollo, Santiago, Chile

ARTICLE INFO

Keywords:
Crowding measures
Global positioning system
SARS-CoV-2
Transport supply

ABSTRACT

Most crowding measures in public transportation are usually aggregated at a service level. This type of aggregation does not help to analyze microscopic behavior such as exposure risk to viruses. To bridge such a gap, our paper proposes four novel crowding measures that might be well suited to proxy virus exposure risk at public transport. In addition, we conduct a case study in Santiago, Chile, using smart card data of the buses system to compute the proposed measures for three different and relevant periods of the COVID-19 pandemic: before, during, and after Santiago's lockdown. We find that the governmental policies diminished public transport crowding considerably for the lockdown phase. The average exposure time when social distancing is not possible passes from 6.39 min before lockdown to 0.03 min during the lockdown, while the average number of encountered persons passes from 43.33 to 5.89. We shed light on how the pandemic impacts differ across various population groups in society. Our findings suggest that poorer municipalities returned faster to crowding levels similar to those before the pandemic.

1. Introduction

The respiratory syndrome coronavirus 2 (SARS-CoV-2), also known as COVID-19, was discovered on December 2019, in Wuhan, China, and declared by The World Health Organization (WHO) as a pandemic in March 2020. Different types of SARS-CoV-2 have been identified (Alkady, ElBahnasy, Leiva, & Gad, 2022). COVID-19 has revolutionized the world's population and economy (Chahuán-Jiménez, Rubilar, De La Fuente-Mella, & Leiva, 2021) forcing us to a new manner of life (Mahdi, Leiva, Mara'Beh, & Martin-Barreiro, 2021). The spread of COVID-19 was so rapid that almost all countries imposed either partial or complete lockdown in affected areas to curb its spread (Li, Zhao, Haitao, Mansourian, & Axhausen, 2021; Ospina, Leite, Ferraz, Magalhães, & Leiva, 2021). Precautionary measures imposed by different governments are directing their masses to follow the standard operating procedure to control its spread (Jerez-Lillo, Álvarez, Gutiérrez, Figueroa-Zúñiga, & Leiva, 2021).

By the end of 2021, the COVID-19 disease infected almost 300 million persons and claimed the lives of more than five million of them worldwide. Both international authorities (such as the WHO) and governments have proposed the implementation of several measures to slow down the virus's spread (Jerez-Lillo et al., 2021). Among others, avoiding public transportation overcrowding has been pointed out as a relevant safety measure to implement. The COVID-19 pandemic disrupted public transport supply and demand quite deeply. For example, public transport providers were forced to cut service span and transport frequencies, whereas ridership dropped sharply due to lockdowns.

☆ Franco Basso gratefully acknowledges the financial support from both the Complex Engineering Systems Institute, ISCI (grant ANID PIA AFB180003) and a grant from the National Agency for Research and Development (ANID) of the Chilean government under the Ministry of Science and Technology, Knowledge and Innovation (FONDECYT Project 11200167). The research of Víctor Leiva was also supported partially by FONDECYT Project 1200525 from ANID. Raúl Pezoa thanks doctoral scholarship to ANID-PFCHA/Doctorado Nacional/2018-21181528. Mauricio Varas thanks a grant from ANID by FONDECYT Project 11190892.

* Corresponding author at: Escuela de Ingeniería Industrial, Pontificia Universidad Católica de Valparaíso, Valparaíso, Chile.
E-mail addresses: francobasso@gmail.com (F. Basso), jonathan.frez@mail.udp.cl (J. Frez), hugo.hernandez.p@mail.pucv.cl (H. Hernández), victorleivasanchez@gmail.com (V. Leiva), raul.pezoa@udp.cl (R. Pezoa), mavaras@udd.cl (M. Varas).

https://doi.org/10.1016/j.scs.2023.104712
Received 10 September 2022; Received in revised form 3 June 2023; Accepted 3 June 2023
Available online 8 June 2023

The reduction in public transport supply affected the match between public transport supply and demand, which could preclude a safe social distancing in public transport buses. In addition, there is a scientific consensus of the airborne transmission of COVID-19 (Morawska & Milton, 2020; Ravindra, Goyal, & Mor, 2021; Vuorinen et al., 2020), whose contagion probability increases depending on the exposure time to the virus (Katal, Wang, & Albettar, 2022; Sun & Zhai, 2020; Ying & O'Clery, 2021). Therefore, it turns relevant to monitor crowding levels in closed spaces, such as public transport buses.

Although several works (Li & Hensher, 2011, 2013) have provided significant contributions to public transport crowding, most of the indicators reported in the literature are often used for transport planning or for determining commuters' quality of service (Tirachini, Hensher, & Rose, 2013). Consequently, they are often aggregated at a bus/train service level, which precludes the understanding of microscopic behaviors at a bus level. Such aggregated indicators allow us, for example, to analyze the impact of crowding on public transport valuation (Tirachini, Hurtubia, Dekker, & Daziano, 2017). However, they are not well suited for studying airborne transmission viruses. Recent technologies, such as automatic passenger counts, image recognition, or weight sensors, provide more disaggregated information, but they are not widely implemented (Dasmalchi, 2020). Thus, to make our calculations, one can employ boarding and alighting information gathered from smart card data, which allows us to study the crowding levels for the whole transport network.

Specifically, in the present paper, we propose four public transport crowding indicators, which seek to serve as a proxy of exposure to airborne viruses. Furthermore, we consider a case study for Santiago, Chile, and its bus public transport system, named Transantiago. The studied period consists of three one-week intervals during 2020: (i) without pandemic; (ii) with pandemic and lockdown; and (iii) with pandemic but without lockdown. Our analysis aims to provide insights about how different factors, such as sociodemographic and spatial variables, impact on the crowding levels of this transportation system.

Therefore, the main objective of our investigation (and consequently our contribution) is to develop and compute novel crowding indicators that might be well suited to be utilized as a proxy of exposure to airborne viruses at public transport. The proposed indicators are: (i) the average time that each bus service line has more than one passenger per square meter; (ii) the average number of passengers per square meter for all buses passing at each bus stop; (iii) the exposure time when social distancing is not possible for each passenger; and (iv) the total number of other people that each passenger meets during his/her trip. These indicators permit us to characterize which services and city zones are the most affected by overcrowding issues, which could be used to develop public policies. These policies include, for example, increasing bus frequency in the most crowded services and/or implementing staggered work hours.

The rest of the paper is structured as follows. Section 2 reviews the state-of-the-art of the relevant literature on the topic. In Section 3, we state the proposed crowding indicators. In Section 4, a case study in Santiago, Chile, is conducted, whereas Section 5 discusses the results obtained in te case study. Finally, Section 6, concludes and points out future research lines.

2. Literature review

The number of standing passengers per square meter is the standard measure for quantifying public transport crowding. However, even though it is widely used by stakeholders around the world (Li & Hensher, 2013), there is no worldwide consensus on the acceptable crowding levels. Threshold values are highly dependent on the countries, ranging from four in Europe (Haywood, Koning, & Monchambert, 2017) to seven in China (Liu & Wen, 2016). In any case, the number of standing passengers per square meter is often not available at a bus level. This is explained due to the lack of proper technology that computes such a measure massively for the whole transport network (Dasmalchi, 2020). This fact implies that, in a COVID-19 era, such aggregated indicators may be inaccurate to measure exposure to the virus although valuable for other purposes.

A well-established line of research focuses on crowding effects in the public transport operations. In this regard, in Tirachini et al. (2013), it was presented a comprehensive literature review of the crowding impact on operating speed, waiting times, travel time reliability, and route and bus choice. In Batarce, Muñoz, and de Dios Ortúzar (2016), it was studied the impact of crowding valuation in both public transport demand and cost–benefit analysis. The authors employed a choice-based preference survey and concluded that the marginal disutility of travel time in crowded vehicles was 2.5 times greater than in buses with available seats. Similarly, in Yap, Cats, and van Arem (2020), it was used revealed preference information gathered from a smart card database, which is similar to the one we use in the present study to evaluate crowding valuation in urban tramways and buses. The results of our work suggest that infrequent travelers do not incorporate expected crowding in their route choice.

Recent technological developments have eased the computing of real-time crowding information (Drabicki, Kucharski, Cats, & Fonzone, 2017). Some efforts have analyzed the impact of sharing this information with public transportation users. For example, in Jenelius (2020), it was proposed a methodology for providing three personalized crowding metrics: (i) the probability of getting a seat onboarding; (ii) the excess perceived travel time compared to uncrowded conditions; and (iii) the expected standing travel time. Among these three metrics, the latter one could be employed for determining COVID-19 risks. In this line, one of the indicators computed in our paper is the expected travel time in which a social distancing of one meter cannot be held. In Wang et al. (2021), it was formulated a bus-focused stochastic model to study the impact of providing real-time bus crowding. The implementation of such a policy could reduce crowding by 25%.

The main problem with the emerging real-time boarding and alighting technologies is their low penetration rate, even in developed countries. For example, in Börjesson and Rubensson (2019), it was argued that, in Sweden, nearly 10% of all buses and trains are equipped with automatic passenger counts (APC) that states the number of boarding and alighting passengers and measures the load factors between stops. Consequently, previous works utilizing these technologies have focused on specific services or bus/train stops, limiting the insights scope. For example, in Zhang, Jenelius, and Kottenhoff (2017), it was analyzed – also in Sweden – the impact of real-time crowding information through a metro pilot study in Stockholm, implemented at a single station. In their work, the authors used the passenger load mass to estimate crowding at trains arriving at the Tekniska Hogskolan station during one week. They found that 25% of the passengers noticed and considered crowding information for their travel decisions. In the same vein, in Kumar, Khani, Lind, and Levin (2021), APC data were employed for studying the potential spread of infectious diseases, such as COVID-19, using passenger encounters. The authors proposed three measures to quantify the encounters risks. Nevertheless, contrary to our study, their simulation results considered one service only. They stated that restricting the maximum number of passengers up to 15 may reduce the potential risk considerably.

Some papers have studied the daily encounters of persons. For example, Sun, Axhausen, Lee, and Huang (2013) studies face-to-face encounters in a city with five million inhabitants. The authors used transit data to understand the dynamics in patterns of social acquaintances and collective human behaviors. Liu, Yin, Ma, Zhang, and Zhao (2020) made the first attempt to study physical encounters in urban metro systems. The authors proposed a method to match passengers to specific trains and measure encounter frequencies and duration in Shenzhen, China. Finally, Mo et al. (2021) proposed a time-varying weighted public transit encounter network to study the spread of infectious disease. The authors conducted a case study in Singapore, finding that

people's preventative behavior is crucial to controlling the spreading of epidemics. Any of these papers focus on defining crowding measures.

The importance of crowding in public transport has recently increased due to the COVID-19 outbreak. Indeed, crowding brings more disutility to passengers than before the pandemic (Cho & Park, 2021), while the value of having a seat while traveling has increased (Aghabayk, Esmailpour, & Shiwakoti, 2021). These changes are one of the reasons that explain the commuting modal shift from public transport to car observed in most cities (Das et al., 2021). Then, different measures have been proposed to reduce public transport overcrowding and mitigate its negative impacts. These measures include flexible work hours (Thomas, Jana, & Bandyopadhyay, 2022), real-time crowding information (Drabicki, Kucharski, Cats, & Szarata, 2021), and redesigning public transportation frequencies (de Weert & Gkiotsalitis, 2021), among others.

Since the beginning of the COVID-19 pandemic, a number of authors have studied the effects of mobility on the spread of the virus, considering the various restriction measures imposed by governments around the world (Jinjarak, Ahmed, Nair-Desai, Xin, & Aizenman, 2020). These articles have focused on studying variations in the movement of people, independent of the mode of transport, using data from various sources such as GPS (Engle, Stromme, & Zhou, 2020; Warren & Skillman, 2020; Zhang et al., 2020) and social networks (Nouvellet et al., 2021; Pérez-Arnal et al., 2021), among others. In general terms, it has been concluded that mobility was significantly reduced (Musselwhite, Avineri, & Susilo, 2020), particularly at the onset of the measures and restrictions imposed by governments to control the pandemic (Kraemer et al., 2020). This decrease in mobility has had an impact on the speed of spread of the virus (Nouvellet et al., 2021).

In this paper, as mentioned, we compute four crowding indicators using smart card data for the full Transantiago system. The data we work with have been employed in previous efforts, for example, to estimate origin–destination matrices (Tamblay, Galilea, Iglesias, Raveau, & Muñoz, 2016) and to infer the trip's purpose (Devillaine, Munizaga, & Trépanier, 2012; Pezoa, Basso, Quilodrán, & Varas, 2023). Other contributions have utilized global positioning system (GPS) data for analyzing several other problems in Santiago, Chile, including commercial bus speed diagnosis (Cortés, Gibson, Gschwender, Munizaga, & Zúñiga, 2011), travel time estimation (Durán-Hormazábal & Tirachini, 2016) and opportunities accessibility (Basso, Frez, Martínez, Pezoa, & Varas, 2020). As we explain in Section 4, it is possible to estimate boarding and alighting using smart card data coupled with GPS data (Munizaga & Palma, 2012). On this, some contributions have used both GPS and smart card data simultaneously for studying crowding. For example, in Arbex and Cunha (2020), the influence of crowding and travel time variability on job opportunities was analyzed. The authors utilized smart card and automatic vehicle location data in Sao Paulo, Brazil, finding a population-weighted average reduction of 56.8% in job accessibility due to crowding discomfort. Furthermore, in Hörcher, Graham, and Anderson (2017), it was also used smart card and vehicle location data to estimate the crowding cost in terms of the equivalent travel time loss in subway transport.

Overall, as also mentioned, to the best of our knowledge, apart from Arbex and Cunha (2020), no previous works have computed crowding indicators at a bus level for a whole transport network. Moreover, even though reducing crowding has been pointed out as crucial for reducing the COVID-19 spread, we are not aware of any contribution that compares public transport crowding during different periods of the COVID-19 pandemic.

3. Methodology

Literature on infection risk establishes a positive correlation between crowding and the risk of COVID-19 contagion. For example, Wiessing et al. (2022) argues that crowding implies prolonged exposure to others, increasing the risk of infection, whereas Collignon (2021) points out that air circulation can be poor in crowded public transportation, making it easier for respiratory droplets to remain in the air and infect others. On this, crowded public transportation often involves touching shared surfaces such as handrails, seat handles, and ticket machines, which can also be a transmission source (Lee & Laefer, 2021). Therefore, by controlling crowding on public transportation, one could expect to restrain the spread of COVID-19 within this transport mode. Nevertheless, no single measure fully characterizes crowding levels (Li & Hensher, 2013), which fosters the development of complementary metrics that allows tracking crowding levels.

Tailored to GPS data, this paper proposes four crowding indicators that could be used as proxies of exposure to airborne viruses. These indicators are computed at different spatial levels (stop, service, and municipality) and take into account different variables (crowding rate, number of people encountered, and exposure time). These indicators complement each other and provide a general overview of the crowding status of the transport network. Overall, the proposed indicators aim to support decision-making for improving the quality of public transport services, especially when social distance is promoted to maintain a safe environment. For instance, the public transportation system in Santiago, Chile relies on contracts with operating companies, whose income is partially determined by compliance indicators such as the supply of seats or the bus headway variability (Tiznado, Galilea, Delgado, & Niehaus, 2014). However, in the post-pandemic context, crowding has become a more relevant attribute of service quality (Cho & Park, 2021), suggesting a need to link operators' income to crowding levels. To achieve this, we believe that the first indicator we propose, computed at a service level, is the relevant measure to evaluate operators' performance. On the other hand, our second proposed indicator, which is computed at the bus stop level, aims to measure the expected level of crowding that users in different zones of the city experience. This information can be useful to transit agencies for designing express services, i.e. bus routes that only stop at a subset of stops (Larrain, Giesen, & Muñoz, 2010), emphasizing stops with the highest expected level of crowding. Finally, during the pandemic, governments worldwide implemented various measures to curb infections. These measures, in the case of Santiago, Chile, included dynamic lockdowns at the municipality level that were applied on a weekly basis (Gramsch, Guevara, Munizaga, Schwartz, & Tirachini, 2022). In this context, we suggest that our third and fourth indicators, computed at the municipality level, could help decision-makers identify which municipalities should be considered for such measures. Moreover, these two indicators could serve as a valuable tool for local authorities, such as mayors, to evaluate whether the public transportation system is meeting the demand for service in their communities, and to determine if additional resources, such as more frequent service or expanded routes are needed.

To compute these indicators, we employ the sets and parameters defined in Tables 1 and 2, respectively. We consider a public transport network consisting of a set S of services. Each service $s \in S$ has a set B_s of bus runs over the studied period. All the bus runs are stored in the set $B = \bigcup_{s \in S} B_s$. Each bus run in the system usually crosses several municipalities, which we denote by the set M. The transport network has a set P of bus stops. For each service $s \in S$, we store its scheduled stops in a set P_s. The set S_p stores the services that stop at $p \in P$.

The average percentage of time that passengers of service s are not able to maintain social distancing is defined as

$$C_s^1 = \frac{\sum_{b \in B_s} \sum_{p \in P_s} t_{sbp} \mathbb{1}_{\left\{ \frac{u_{sbp}}{l_b} > h \right\}}}{\sum_{b \in B_s} \sum_{p \in P_s} t_{sbp}}, \tag{1}$$

where $\mathbb{1}$ is the indicator function and the other notations being stated in Tables 1 and 2. The situation represented in (1) occurs when the number of passengers per square meter, u_{sbp}/l_b namely, is greater than a specific threshold h, which was set at one in this work.

Table 1
Sets used for the computation of crowding indicators.

Notation	Definition
B	Set of bus runs
S	Set of services
P	Set of bus stops
M	Set of municipalities
J	Set of trips
B_s	Set of bus runs providing service $s \in S$
S_p	Set of services stopping at bus stop $p \in P$
P_s	Set of bus stops of service $s \in S$

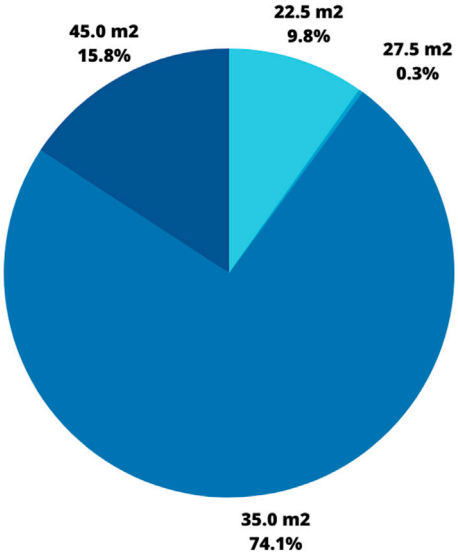

Fig. 1. Floor surface distribution of Transantiago fleet.

The average crowding level of buses stopping at bus stop p, in passenger per square meter is formulated as

$$C_p^2 = \frac{\sum_{s \in S_p} \sum_{b \in B_s} \frac{u_{sbp}}{l_b}}{\sum_{s \in S_p} \sum_{b \in B_s} |B_s|}, \tag{2}$$

where $|B_s|$ is the number of the bus runs providing service, with $s \in S$, and whose notations are established in Tables 1 and 2. The indicator defined in (2) can be interpreted as the expected crowding level that a passenger waiting for a bus in stop p will face.

The average time a person that starts its trip in municipality m will not be able to keep social distancing while using public transport is expressed as

$$C_m^3 = \frac{\sum_{j \in J} \sum_{s \in S} \sum_{b \in B_s} \sum_{p \in P_s} \beta_{jm}\, \alpha_{jsbp}\, t_{sbp}\, \mathbb{1}\left\{\frac{u_{sbp}}{l_b} > h\right\}}{\sum_{j \in J} \beta_{jm}}, \tag{3}$$

whose notations are given in Tables 1 and 2. The indicator stated in (3) is related to both the crowding level of public transport and the travel time.

The average number of people that a passenger will meet during his/her journey, for trips that start in municipality m, is represented as

$$C_m^4 = \frac{\sum_{j \in J} \sum_{s \in S} \sum_{b \in B_s} \sum_{p \in P_s} \beta_{jm} \gamma_{jp} u_{sbp} + \sum_{j \in J} \sum_{s \in S} \sum_{b \in B_s} \sum_{p \in P_s} \beta_{jm} \alpha_{jsbp} (1 - \gamma_{jp}) v_{sbp}}{\sum_{j \in J} \beta_{jm}}, \tag{4}$$

whose notations are given in Tables 1 and 2. The numerator stated in (4) corresponds to the number of passengers already on the bus when a random passenger boards it. In contrast, the denominator corresponds to the number of passengers that board during the rest of his/her journey.

On the one hand, note that the indicators defined in (1) and (2) focus on the trade-off between demand and supply of the public transport system, analyzing the same phenomena from two angles, namely, buses and bus stops. On the other hand, the indicators stated in (3) and (4) focus on the impact of crowding at an individual level. On this, both indicators depend on the trip's starting municipality. Thus, they are influenced by the spatial distribution of works and households.

4. Case study for Santiago, Chile

Next, we describe the data employed in our research. We analyze how public transport crowding indicators vary during the different stages of the COVID-19 mobility restrictions in Santiago. To make our calculations, we consider three periods, all in the morning rush from 7:00 to 8:00 h. The first period is 9–13 March 2020, when the WHO declared COVID-19 outbreak a global pandemic and before the Chilean government took preventive measures. The second period is 6–10 July 2020, when Santiago was in full lockdown. Only essential activities, such as healthcare and food supply, were operating during this period. In addition, the third period is 9–13 November 2020, when there was no lockdown during the business days. Santiago was in lockdown on weekends only in this stage, and the nighttime curfew remained in place the whole week.

The proposed methodology uses two data sources to compute the crowding indicators: (i) bus features and (ii) smart card database. All of these data were provided by the "Directorio de Transporte Público Metropolitano" (DTPM, in Spanish) www.dtpm.cl, the government authority in charge of Transantiago operations. In what follows, we describe both sources in further detail.

Our methodology involves tracking each bus, estimating the number of passengers on board, and dividing it by the bus floor surface. On this, Table 3 reports the bus information gathered from the DTPM. In particular, both the license plate and bus length are essential inputs since, as opposed to most previous contributions, our focus lies in estimating crowding indicators using disaggregated data at a bus level. The database has 6978 entries, each corresponding to a specific bus. In this case, buses are categorized into four groups depending on their floor surfaces, which distribution is shown in Fig. 1.

Now, we describe the smart card database. In Transantiago, on the one hand, only boarding date are recorded. The alighting data, on the other hand, are estimated by Transantiago authorities using "Análisis de datos de transporte público" (ADATRAP, in Spanish) executed by the DTPM www.dtpm.cl/index.php/documentos/matrices-de-viaje, a software that implements the procedure proposed in Munizaga and Palma (2012). This software combines boarding and GPS data to identify an alighting position. The database we received, whose fields are shown in Table 4, contains the position and time of both boarding and alighting bus stop as well as data related to the service line employed by the passenger. Nonetheless, it was not possible to estimate alighting for every transaction. This last is reflected in the field "has alighting" of the database, which takes value one if it is possible to estimate an alighting point, and zero otherwise. The database used in this research has 36,343,343 entries: 21,480,007 for the first period; 3,490,541 for the second one; and 11,372,795 for the third period. Of these entries, 74.12% have an estimated alighting point. For the boarding data points without alighting information, we assign the bus stops proportionally to the rest of the entries for each service. Fig. 2 depicts the transactions' distribution for the three studied periods, showing a sharp decrease in public transport utilization for the full lockdown period and a subsequent increase when restrictions are lifted. In the present study, we analyze how these reductions in public transport demand impacted the crowding levels. Note that the conclusion is not straightforward since crowding is not determined only by demand, but also by public transport supply patterns.

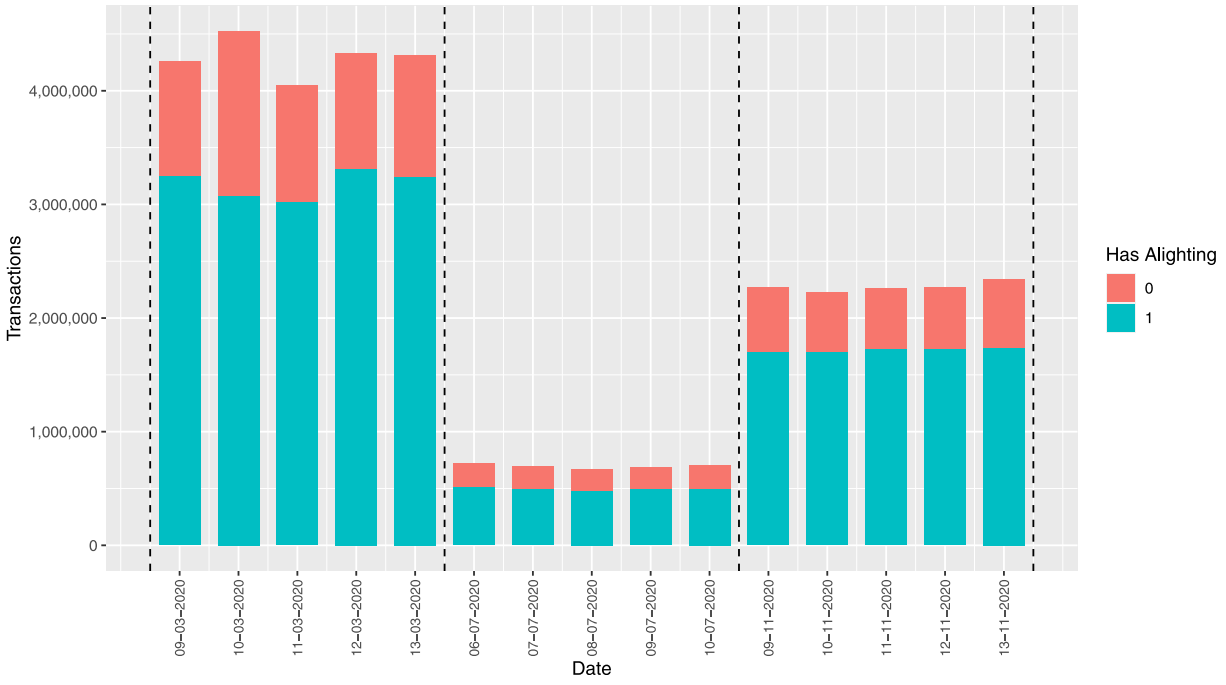

Fig. 2. Distribution of transactions in the three study periods.

Table 2
Parameters used for the computation of crowding indicators.

Notation	Definition
h	Maximum acceptable number of passengers per square meter
l_b	Floor surface of bus $b \in B$
u_{sbp}	Estimated number of passengers in the bus run $b \in B_s$ of service $s \in S$ at bus stop $p \in P_s$
v_{sbp}	Estimated number of passengers boarding the bus run $b \in B_s$ of service $s \in S$ at bus stop $p \in P_s$
t_{sbp}	Travel time for the bus run $b \in B_s$ of service $s \in S$ from bus stop $p \in P_s$ to the next one
α_{jsbp}	1 if trip $j \in J$ passes by bus stop $p \in P_s$ for the bus run $b \in B_s$ of service $s \in S$, 0 otherwise
β_{jm}	1 if trip $j \in J$ starts in municipality $m \in M$, 0 otherwise
γ_{jp}	1 if trip $j \in J$ starts at bus stop $p \in P$, 0 otherwise

Table 3
Bus features information.

Field	Example
License plate	BBJZ70
Brand	Mercedes Benz
Model	LO 915
Year of production	2008
Number of seats	56
Bus type	A1
Bus length	9 m
Emission standards	EURO III

Table 4
Smart card information.

Field	Example
Has alighting	1
Boarding time	2020-03-07 08:50:59
Alighting time	2020-03-07 09:12:53
Segment time [seconds]	1314
x boarding [UTM]	348 652
y boarding [UTM]	6 303 586
x alighting [UTM]	342 840
y alighting [UTM]	6 304 215
Service line boarding	B01 00I
Bus stop boarding	L-4-18-120-OP
Bus stop alighting	L-2-21-5-OP
Municipality boarding	RECOLETA
Municipality alighting	CONCHALI
License plate	CJJT64

5. Results and discussion

In this section, we present and discuss the results obtained by computing the indicators defined in Section 3 using the data described in Section 4.

5.1. C_s^1 indicator

Table 5 reports several descriptive statistics for C_s^1, the average percentage of time that passengers of service s are not able to maintain social distancing, defined in (1) considering three specific periods: March 2020, June 2020 and November 2020. First, note that the full lockdown imposed on June 2020 positively impacts crowding, diminishing it by 94.6%. During November 2020, however, as some non-essential activities restarted, the crowding levels increased, attaining a reduction of 62.3% compared to March 2020. These results are somewhat consistent with the cellphones data-based mobility analysis described in ISCI (2020), where is shown that the mobility reduced 35.9% in July 2020 and 22.4% in November 2020, compared to March 2020. Yet, the reduction value is greater for C_s^1 compared to the results reported in ISCI (2020). This difference might be explained since the cellphone data consider all movements in the city independently of the transport mode, while C_s^1 considers public transport mode only. These

Table 5
Descriptive statistics for the average percentage of time that passengers of service s are not able to maintain social distancing (C_s^1).

Period	Mean	Standard deviation	1st quartile	Median	3rd quartile	Mean top ten
March 2020	15.68	19.24	0.00	8.01	27.48	76.05
June 2020	0.84	3.51	0.00	0.00	0.00	22.61
November 2020	5.91	10.95	0.00	0.00	7.55	50.46

findings support some recent evidence that shows an increase in private transport use compared to public transport (Das et al., 2021).

5.2. C_2^p indicator

Now, consider Fig. 3, which shows the results for the average crowding level of buses stopping at bus stop p, in passenger per square meter, namely C_p^2, defined in (2). Before the pandemic started, there were multiple areas of Santiago with significant crowding levels, attaining up to three passengers per square meter on average. These zones are mainly located in some municipalities of the center of the region (Santiago and Estación Central), southeast (Puente Alto and La Florida), and western part of the city (Pudahuel and Maipú).

When the full lockdown was in place, as Fig. 3(b) shows, crowding levels decrease everywhere in the city as a result of the reduced supply and a sharp decrease in demand. Nevertheless, there are still some sectors, mainly in the southeast (Puente Alto and La Florida), where residents still face high levels of crowding. Also, in November 2020, all the municipalities in Santiago did not have mobility restrictions, yet other restrictions remain (for example, curfew and limited capacity on shops). The relaxation of the measures imply an increase of crowding level in some specific areas such as the neighborhood of Alameda street from the downtown to the west, Cerrillos, La Granja and Las Condes.

Fig. 4 shows the difference in the C_p^2 indicator between all the pairs of studied months. When this difference is negative (respectively, positive), that is, when there is a reduction (respectively, increase) in the crowding indicator, the hexagon is colored in green (respectively, red). As we can observe in Fig. 4(a), the most important reductions occurred in the northeast part of the city, attaining over 90% of reduction in some cases. These zones correspond to the wealthier municipalities of Santiago (Las Condes, Vitacura, and Lo Barnechea). On the contrary, the lowest reductions occurred in the west part of the city, in which a large number of workers reside. A similar pattern is presented in Fig. 4(b), but with less values since several commercial activities restarted. Furthermore, Fig. 4(c) shows that, in November, the wealthier municipalities recovered some of their public transport activities.

5.3. C_m^3 and C_m^4 indicators

Table B.1 reports the resulting values for indicators C_m^3 corresponding to the average time a person that starts its trip in municipality m will not be able to keep social distancing while using public transport, and C_m^4 corresponding to the average number of people that a passenger will meet during his/her journey, for trips that start in municipality m. These two indicator are defined in (3) and (4), respectively. Consistent with the previous results, there is a significant decrease in both indicators during July 2020 compared to March 2020. The average virus exposure time faced by a commuter $\sum_{m\in M} C_m^3/|M|$ passes from 6.39 min to 0.03 min, where $|M|$ is the number of municipalities, with $m \in M$, while the average number of encountered persons $\sum_{m\in M} C_m^4/|M|$ passes from 46.14 to 15.53. The average travel time, T namely, reduces by 27.35%, mostly explained by the significant decrease in traffic congestion. Also, we can observe that variability for both indicators and the travel time is considerably reduced. For example, the difference between the minimum and maximum values for the number of encountered persons in March 2020 is 43.33, while in July 2020 is only 5.89. In November 2020, when lockdown restrictions were lifted, there was an increase in all the crowding indicator levels. In particular, the average number of encountered persons grew for every municipality, although not homogeneously. Indeed, we find a correlation of −0.39 between the average municipality income and the increase in the number of encountered persons in November compared to July 2020. This last shows that poorer municipalities returned faster to crowding levels similar to those before the pandemic. Such a result is in line with an online questionnaire conducted by the "Instituto Sistemas Complejos de Ingeniería" (ISCI, in Spanish) www.isci.cl during march 2020, that shows huge inequalities in people working at home depending on their monthly salary (Fig. A.1). These findings are similar to those obtained in other studies performed in different countries and using different data (e.g, Long & Ren, 2022).

To assess the significance of the relations, we build a linear regression model, considering as dependent variable C_{mt}, which might correspond either to indicator C_m^3 or C_m^4 during period t. As independent variables, firstly we consider x_m, which corresponds to the average income for inhabitants of municipality m (in Chilean Pesos). The values for this last variable is gathered from the National Statistics Institute.[1] Secondly, we consider z_t and w_m as dummy control variables for each period and municipality, respectively. Eq. (5) shows the mathematical expression of the model, while the results are shown in Table 6.

$$C_{mt} = \alpha + \beta x_m + \delta_t z_t + \eta_m w_m + \epsilon_{mt} \tag{5}$$

Several conclusions can be drawn from Table 6. First, we observe that the parameters for both dummy variables for the second and third periods are statistically significant and negative for both models. This means that the measures taken by the government had a significant effect on the average exposure time and the average number of persons encountered compared to the pre-pandemic situation, implying a ceteris paribus reduction in the indicator C_m^3 of 6.36 and 5.50 min for second and third periods, respectively. Furthermore, the reduction in the indicator C_m^4 can be quantified as 30.61 and 17.18 persons encountered for second and third periods, respectively.

Regarding the socio-economic effects, we conclude that there is a statistically significant negative relationship between the average income and both indicators. By analyzing the value of the estimated parameters, we find that an increase of one million Chilean pesos (approximately 1250 USD) in the average monthly salary leads to a reduction of 2.36 min of exposure time and 10.65 encountered persons, after controlling for all other covariates.

6. Concluding remarks

Crowding is a relevant topic in public transportation literature due to its vast impact on quality of service and operational costs. During the COVID-19 pandemic, this relevance has grown since one of the main ways to prevent the spread of the virus is to keep social distancing. Indeed, recent efforts have shown an increased passengers' perceived disutility of public transport crowding during the COVID-19 outbreak (Aghabayk et al., 2021; Cho & Park, 2021). Unfortunately, there is no scientific consensus on how crowding should be measured or which are its acceptable levels.

Traditional crowding measures consider the average number of persons per square meter but are usually aggregated at a service level. This type of aggregation is not suitable for analyzing microscopic behavior

[1] https://www.ine.gob.cl/estadisticas/sociales/ingresos-y-gastos/encuesta-suplementaria-de-ingresos.

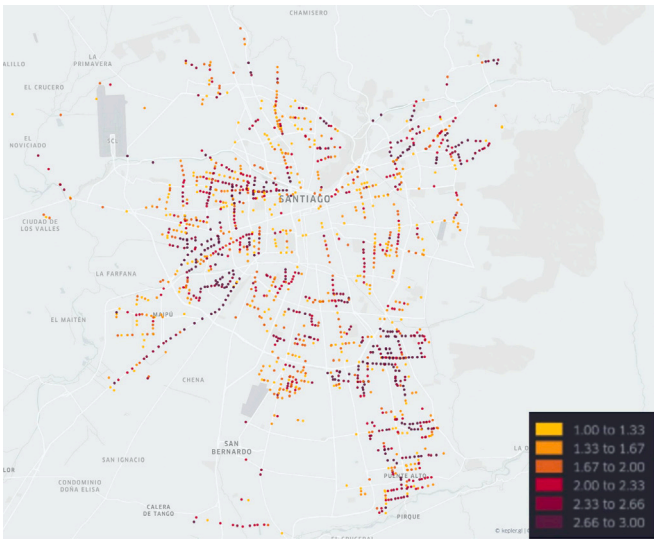

(a) March 2020.

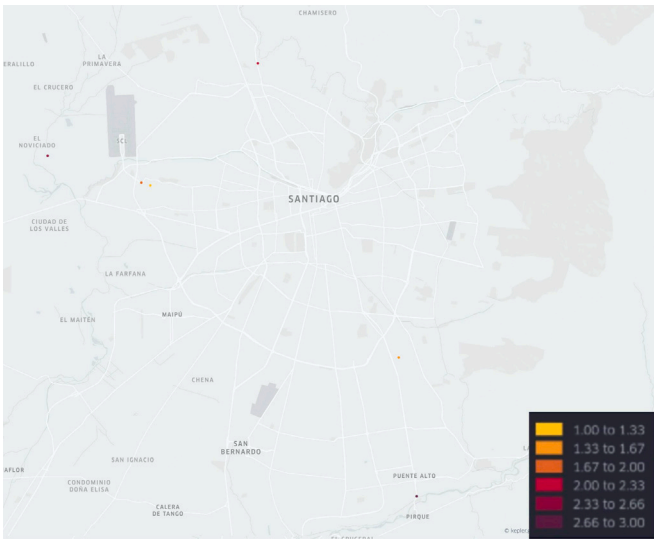

(b) June 2020.

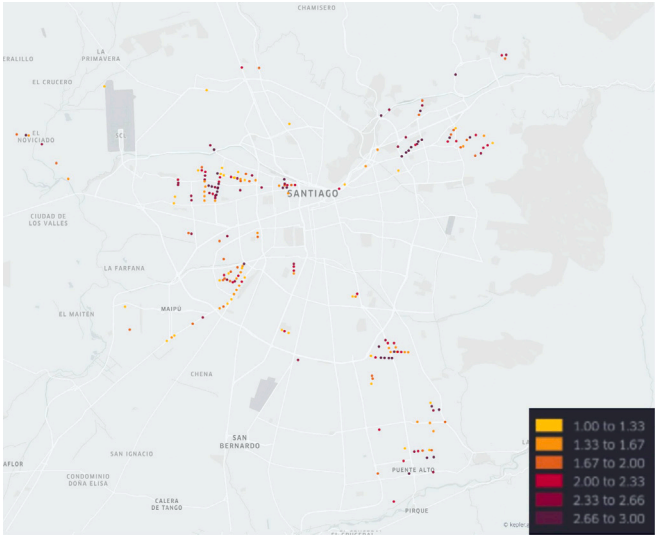

(c) November 2020.

Fig. 3. Average crowding [pax/m^2] for all the buses passing each bus stop (C_p^2).

Table 6
Results of the linear regression model (for the sake of exposition, the coefficient of municipality dummy variables are omitted). DF: degree of freedom.

Variable	Estimate	Model for C_m^3 Std. Error	p-value	Estimate	Model for C_m^4 Std. Error	p-value
Intercept	9.698e+00	1.464e+00	7.57e−09***	5.917e+01	4.664e+00	<2e−16***
Average Income	−2.368e−06	1.101e−06	0.0351*	−1.065e−05	3.506e−06	0.00343**
Period2	−6.359e+00	4.131e−01	<2e−16***	−3.061e+01	1.316e+00	<2e−16***
Period3	−5.495e+00	4.131e−01	<2e−16***	−1.718e+01	1.316e+00	<2e−16***
Residual standard error:	1.703 (66 DF)			5.425 (66 DF)		
Adjusted R-squared:	0.8312			0.9083		
F-statistic:	9.286 (35 and 66 DF)		9.636e−15***	18.67 (35 and 66 DF)		<2e−16***

such as exposure to COVID-19. To bridge this gap, we have proposed four crowding indicators that aim to be good proxies of virus risk exposure. The distinctive feature of these indicators is that they can be computed at a bus level so microscopic analyses may be performed. To illustrate the proposed indicators, we have conducted a case study using smart card data from the public transportation services in Santiago, Chile. We have computed and compared the four crowding indicators during three different periods: before the pandemic started, during, and

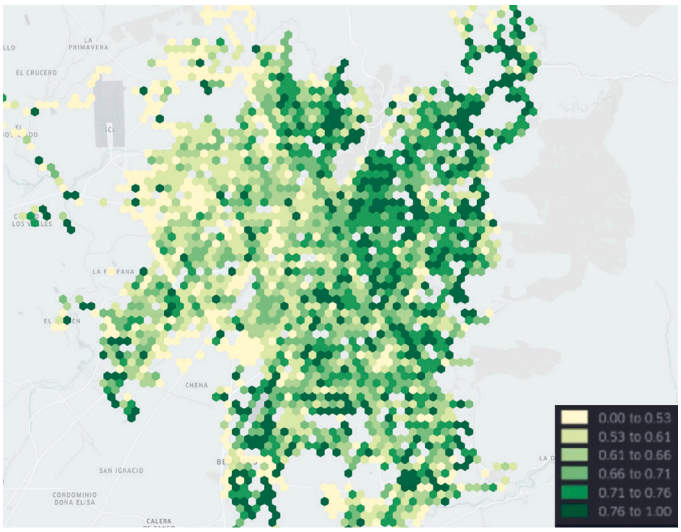

(a) $C_p^2[\text{July}] - C_p^2[\text{March}]$

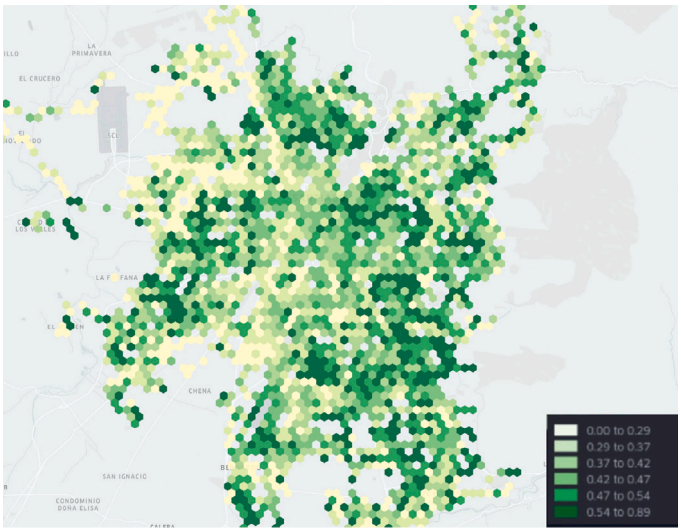

(b) $C_p^2[\text{November}] - C_p^2[\text{March}]$

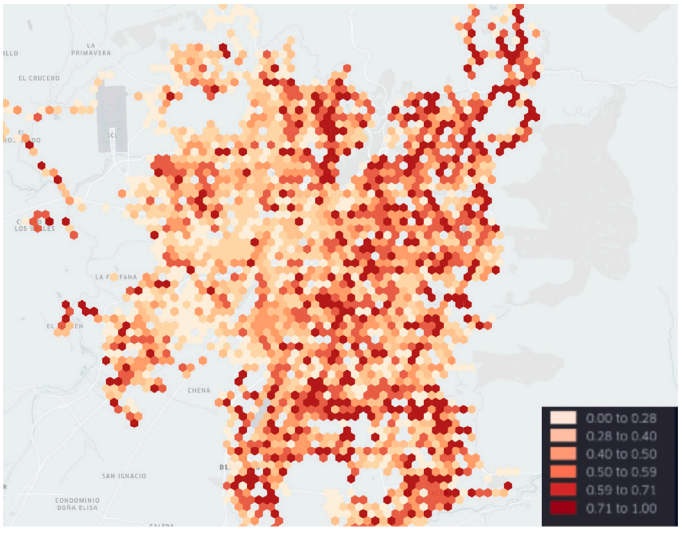

(c) $C_p^2[\text{November}] - C_p^2[\text{July}]$

Fig. 4. Changes for C_p^2 [pax/m^2], the average crowding level of buses stopping at bus stop p, for the three studied periods.

after Santiago's lockdown. To the best of our knowledge, this is the first effort in which crowding indicators are computed at such disaggregated levels in Santiago, Chile.

The application of the devised methodology allowed us to determine whether the mobility restrictions were able to reduce crowding indicators. In the case of Santiago, Chile, we have found that the governmental policies diminished public transport crowding considerably during the lockdown phase. For example, a commuter's average virus exposure time passed from 6.39 min in March 2020 to 0.03 min in July 2020, while the average number of encountered persons passed from 43.33 to 5.89. After the lockdown finished, some crowding reappeared. Nevertheless, these increases were not homogeneous in the city. In November 2020, the most crowded buses were concentrated in the west and south part of the city where the poorer people live.

The proposed methodology has multiple practical applications beyond the COVID-19 pandemic. Our results could help policymakers to focus their efforts and resources on those zones and bus services with worse crowding levels even in a no COVID-19 situation. Decision-makers can employ information from our public transportation crowding indicators to draw conclusions about the capacity and efficiency of the system and identify areas for improvement. This information can be used to make informed decisions about the design, implementation, and/or management of public transportation systems. For example, if crowding indicators show high levels of overcrowding, decision-makers may invest in additional public transport capacity or improve the current service's efficiency. Similarly, if congestion indicators show low ridership, decision-makers may reduce service frequency or extend the network's reach.

The application of our proposed methodology could also impact the demand for public transport. In fact, since literature supports the benefits of making available real-time crowding information, the computation and public diffusion of our crowding indicators may help to reduce the crowding levels by producing a more equilibrated utilization of public transport capacity (Drabicki et al., 2021). This reallocation

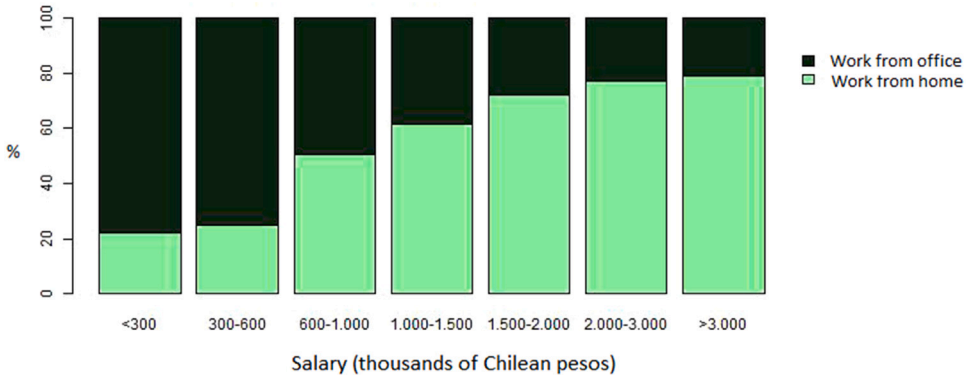

Fig. A.1. Percentage of people working at home. Source: ISCI www.uchile.cl/noticias/162383/solo-1-de-cada-4-trabajadores-de-menores-ingresos-realizo-teletrabajo (in Spanish). Accessed on February 2022.

Table B.1
Average exposure time (C_m^3), average number of encountered persons (C_m^4), and average travel time (T) by commuters starting their trip in municipality m during a public transport journey for the indicated periods.

Municipality (m)	March 2020			July 2020			November 2020		
	C_m^3	C_m^4	T	C_m^3	C_m^4	T	C_m^3	C_m^4	T
Cerrillos	11.31	56.42	52.11	0.07	15.63	35.56	2.18	41.12	45.81
Cerro Navia	11.91	76.31	61.21	0.01	16.35	42.53	3.04	54.69	53.00
Conchalí	4.25	39.85	55.38	0.00	14.60	36.02	0.43	23.94	49.22
El Bosque	4.61	41.87	54.19	0.00	16.41	36.53	0.65	25.29	50.73
Estación Central	5.75	40.85	43.82	0.04	16.08	33.19	0.97	29.36	39.75
Huechuraba	4.54	41.86	55.94	0.02	14.33	34.94	0.39	22.57	51.30
Independencia	3.89	41.12	47.54	0.01	14.83	36.94	1.47	35.30	42.87
La Cisterna	4.30	35.31	43.25	0.02	15.09	36.46	0.74	23.05	39.00
La Florida	9.25	55.61	53.82	0.02	15.40	41.88	1.00	29.97	47.59
La Granja	6.71	50.12	50.81	0.00	15.04	34.13	0.60	26.28	46.06
La Pintana	4.99	43.00	59.56	0.04	14.41	35.45	0.63	25.61	53.19
La Reina	5.54	47.96	51.88	0.02	17.84	33.65	0.27	23.28	49.01
Las Condes	4.24	38.16	52.97	0.00	12.05	39.53	0.37	19.55	47.38
Lo Barnechea	5.54	40.97	72.91	0.08	17.87	45.95	0.15	18.12	65.13
Lo Espejo	5.68	53.68	48.82	0.04	17.42	35.78	0.81	34.10	45.26
Lo Prado	5.93	37.03	45.38	0.05	15.08	35.86	0.93	27.69	42.13
Macul	8.24	49.61	46.82	0.01	15.19	29.96	0.53	27.17	41.68
Maipú	18.66	66.65	69.24	0.03	15.76	52.52	1.34	36.92	58.19
Ñuñoa	4.94	38.74	42.80	0.00	13.72	35.42	0.51	23.33	38.24
Pedro Aguirre Cerda	5.26	47.93	43.63	0.06	15.09	31.99	0.86	33.79	39.80
Peñalolén	4.77	48.26	52.64	0.00	14.74	40.79	0.34	30.84	46.97
Providencia	5.25	38.68	42.84	0.03	15.75	35.01	0.57	22.93	38.80
Pudahuel	9.79	53.88	57.94	0.07	16.40	41.15	1.10	37.65	51.44
Puente Alto	7.35	50.24	66.17	0.04	14.84	55.35	1.21	30.41	59.55
Quilicura	7.02	45.85	66.71	0.03	15.37	48.98	2.49	37.83	61.68
Quinta Normal	10.01	62.23	47.91	0.02	16.33	33.18	1.62	40.68	43.99
Recoleta	3.32	32.98	46.61	0.09	15.52	35.33	0.39	20.27	43.12
Renca	6.67	55.23	55.31	0.00	14.95	36.00	1.25	39.90	49.26
San Bernardo	3.73	37.97	61.81	0.02	14.09	46.24	0.67	24.42	55.16
San Joaquín	5.11	43.11	44.22	0.00	15.32	31.96	0.57	26.68	38.79
San Miguel	4.16	37.66	40.17	0.12	17.00	34.04	0.62	23.54	37.34
San Ramón	5.60	42.49	50.09	0.14	17.94	35.54	0.71	24.22	45.37
Santiago	4.77	38.52	37.90	0.06	16.60	32.66	0.88	25.29	34.52
Vitacura	4.29	38.74	55.04	0.00	15.07	40.82	0.29	19.01	48.80

occurs because when users have more real-time crowding information, they may be able to switch to other services, improving their travel experience and that of others. We think this is feasible since our computations are based on GPS and smart card data, which might be available online. In addition, a user-friendly app could help commuters in their journeys and serve as a building block for a more sophisticated real-time crowding information system.

Even though we expect that the number of COVID-19 cases will reduce next year, seasonal airborne transmission viruses will remain. Thus, more work in disaggregated crowding indicators research is definitely needed. Our proposed methodology can be employed to measure crowding levels at a specific moment. Nonetheless, it is not clear which are the best paths to follow when improving this situation. Therefore, more research is required to analyze specific measures, such as staggered working hours or supply increases. Implementing these policies could persuade commuters to utilize public transport again after the historical demand reduction during the COVID-19 pandemic.

Declaration of competing interest

The authors declare no conflicts of interest.

Data availability

Data will be made available on request.

Acknowledgments

Franco Basso gratefully acknowledges the financial support from both the Complex Engineering Systems Institute, ISCI (grant ANID PIA AFB180003) and a grant from the National Agency for Research and Development (ANID) of the Chilean government under the Ministry of Science and Technology, Knowledge and Innovation (FONDECYT Project 11200167). The research of Víctor Leiva was also supported partially by FONDECYT Project 1200525 from ANID. Raúl Pezoa thanks doctoral scholarship to ANID-PFCHA/Doctorado Nacional/2018-21181528. Mauricio Varas thanks a grant from ANID by FONDECYT Project 11190892.

Appendix A. Telework in Chile

See Fig. A.1.

Appendix B. Detailed results for C_m^3 and C_m^4 indicators

See Table B.1.

References

Aghabayk, K., Esmailpour, J., & Shiwakoti, N. (2021). Effects of COVID-19 on rail passengers' crowding perceptions. *Transportation Research Part A: Policy and Practice*, *154*, 186–202.

Alkady, W., ElBahnasy, K., Leiva, V., & Gad, W. (2022). Classifying COVID-19 based on amino acids encoding with machine learning algorithms. *Chemometrics and Intelligent Laboratory Systems*, *224*, Article 104535.

Arbex, R., & Cunha, C. B. (2020). Estimating the influence of crowding and travel time variability on accessibility to jobs in a large public transport network using smart card big data. *Journal of Transport Geography*, *85*, Article 102671.

Basso, F., Frez, J., Martínez, L., Pezoa, R., & Varas, M. (2020). Accessibility to opportunities based on public transport gps-monitored data: The case of Santiago, Chile. *Travel Behaviour and Society*, *21*, 140–153.

Batarce, M., Muñoz, J. C., & de Dios Ortúzar, J. (2016). Valuing crowding in public transport: Implications for cost-benefit analysis. *Transportation Research Part A: Policy and Practice*, *91*, 358–378.

Börjesson, M., & Rubensson, I. (2019). Satisfaction with crowding and other attributes in public transport. *Transport Policy*, *79*, 213–222.

Chahuán-Jiménez, K., Rubilar, R., De La Fuente-Mella, H., & Leiva, V. (2021). Breakpoint analysis for the COVID-19 pandemic and its effect on the stock markets. *Entropy*, *23*(1), 100.

Cho, S.-H., & Park, H.-C. (2021). Exploring the behaviour change of crowding impedance on public transit due to COVID-19 pandemic: before and after comparison. *Transportation Letters*, *13*(5–6), 367–374.

Collignon, P. (2021). COVID-19 and future pandemics: is isolation and social distancing the new norm? *Internal Medicine Journal*, *51*(5), 647–653.

Cortés, C. E., Gibson, J., Gschwender, A., Munizaga, M., & Zúñiga, M. (2011). Commercial bus speed diagnosis based on GPS-monitored data. *Transportation Research Part C (Emerging Technologies)*, *19*(4), 695–707.

Das, S., Boruah, A., Banerjee, A., Raoniar, R., Nama, S., & Maurya, A. K. (2021). Impact of COVID-19: A radical modal shift from public to private transport mode. *Transport Policy*, *109*, 1–11.

Dasmalchi, E. (2020). Using real-time crowding data as a rider communication strategy in the COVID-19 pandemic.

de Weert, Y., & Gkiotsalitis, K. (2021). A covid-19 public transport frequency setting model that includes short-turning options. *Future Transportation*, *1*(1), 3–20.

Devillaine, F., Munizaga, M., & Trépanier, M. (2012). Detection of activities of public transport users by analyzing smart card data. *Transportation Research Record*, *2276*(1), 48–55.

Drabicki, A., Kucharski, R., Cats, O., & Fonzone, A. (2017). Simulating the effects of real-time crowding information in public transport networks. In *2017 5th IEEE international conference on models and technologies for intelligent transportation systems (MT-ITS)* (pp. 675–680). IEEE.

Drabicki, A., Kucharski, R., Cats, O., & Szarata, A. (2021). Modelling the effects of real-time crowding information in urban public transport systems. *Transportmetrica A: Transport Science*, *17*(4), 675–713.

Durán-Hormazábal, E., & Tirachini, A. (2016). Estimation of travel time variability for cars, buses, metro and door-to-door public transport trips in Santiago, Chile. *Research in Transportation Economics*, *59*, 26–39.

Engle, S., Stromme, J., & Zhou, A. (2020). Staying at home: mobility effects of covid-19. Available At SSRN 3565703.

Gramsch, B., Guevara, C. A., Munizaga, M., Schwartz, D., & Tirachini, A. (2022). The effect of dynamic lockdowns on public transport demand in times of COVID-19: Evidence from smartcard data. *Transport Policy*, *126*, 136–150.

Haywood, L., Koning, M., & Monchambert, G. (2017). Crowding in public transport: Who cares and why? *Transportation Research Part A: Policy and Practice*, *100*, 215–227.

Hörcher, D., Graham, D. J., & Anderson, R. J. (2017). Crowding cost estimation with large scale smart card and vehicle location data. *Transportation Research, Part B (Methodological)*, *95*, 105–125.

ISCI (2020). Reporte de movilidad nacional noviembre 2020. URL: https://isci.cl/wp-content/uploads/2020/11/Reporte-de-Movilidad-Nacional-NOVIEMBRE-2020.pdf, Accessed on 29/06/2021.

Jenelius, E. (2020). Personalized predictive public transport crowding information with automated data sources. *Transportation Research Part C (Emerging Technologies)*, *117*, Article 102647.

Jerez-Lillo, N., Álvarez, B. L., Gutiérrez, J. M., Figueroa-Zúñiga, J. I., & Leiva, V. (2021). A statistical analysis for the epidemiological surveillance of COVID-19 in Chile. *Signa Vitae*, *18*(2), 19–31.

Jinjarak, Y., Ahmed, R., Nair-Desai, S., Xin, W., & Aizenman, J. (2020). Accounting for global COVID-19 diffusion patterns, January–April 2020. *Economics of Disasters and Climate Change*, *4*(3), 515–559.

Katal, A., Wang, L. L., & Albettar, M. (2022). A real-time web tool for monitoring and mitigating indoor airborne COVID-19 transmission risks at city scale. *Sustainable Cities and Society*, *80*, Article 103810.

Kraemer, M. U., Yang, C.-H., Gutierrez, B., Wu, C.-H., Klein, B., Pigott, D. M., et al. (2020). The effect of human mobility and control measures on the COVID-19 epidemic in China. *Science*, *368*(6490), 493–497.

Kumar, P., Khani, A., Lind, E., & Levin, J. (2021). Estimation and mitigation of epidemic risk on a public transit route using automatic passenger count data. *Transportation Research Record*, *2675*(5), 94–106.

Larrain, H., Giesen, R., & Muñoz, J. C. (2010). Choosing the right express services for bus corridor with capacity restrictions. *Transportation Research Record*, *2197*(1), 63–70.

Lee, S. K., & Laefer, D. (2021). Spring 2020 COVID-19 community transmission behaviours around New York city medical facilities. *Infection Prevention in Practice*, *3*(3), Article 100158.

Li, Z., & Hensher, D. A. (2011). Crowding and public transport: A review of willingness to pay evidence and its relevance in project appraisal. *Transport Policy*, *18*(6), 880–887.

Li, Z., & Hensher, D. A. (2013). Crowding in public transport: a review of objective and subjective measures. *Journal of Public Transportation*, *16*(2), 6.

Li, A., Zhao, P., Haitao, H., Mansourian, A., & Axhausen, K. W. (2021). How did micro-mobility change in response to COVID-19 pandemic? A case study based on spatial-temporal-semantic analytics. *Computers, Environment and Urban Systems*, *90*, Article 101703.

Liu, J., & Wen, H. (2016). Public transport crowding valuation: Evidence from college students in Guangzhou. *Journal of Public Transportation*, *19*(3), 5.

Liu, K., Yin, L., Ma, Z., Zhang, F., & Zhao, J. (2020). Investigating physical encounters of individuals in urban metro systems with large-scale smart card data. *Physica A*, *545*, Article 123398.

Long, J. A., & Ren, C. (2022). Associations between mobility and socio-economic indicators vary across the timeline of the Covid-19 pandemic. *Computers, Environment and Urban Systems*, *91*, Article 101710.

Mahdi, E., Leiva, V., Mara'Beh, S., & Martin-Barreiro, C. (2021). A new approach to predicting cryptocurrency returns based on the gold prices with support vector machines during the COVID-19 pandemic using sensor-related data. *Sensors*, *21*(18), 6319.

Mo, B., Feng, K., Shen, Y., Tam, C., Li, D., Yin, Y., et al. (2021). Modeling epidemic spreading through public transit using time-varying encounter network. *Transportation Research Part C (Emerging Technologies)*, *122*, Article 102893.

Morawska, L., & Milton, D. K. (2020). It is time to address airborne transmission of coronavirus disease 2019 (COVID-19). *Clinical Infectious Diseases*, *71*(9), 2311–2313.

Munizaga, M. A., & Palma, C. (2012). Estimation of a disaggregate multimodal public transport origin–destination matrix from passive smartcard data from santiago, Chile. *Transportation Research Part C (Emerging Technologies)*, *24*, 9–18.

Musselwhite, C., Avineri, E., & Susilo, Y. (2020). Editorial JTH 16–The Coronavirus Disease COVID-19 and implications for transport and health. *Journal of Transport & Health*, *16*, Article 100853.

Nouvellet, P., Bhatia, S., Cori, A., Ainslie, K. E., Baguelin, M., Bhatt, S., et al. (2021). Reduction in mobility and COVID-19 transmission. *Nature communications*, *12*(1), 1–9.

Ospina, R., Leite, A., Ferraz, C., Magalhães, A., & Leiva, V. (2021). Data-driven tools for assessing and combating COVID-19 outbreaks in Brazil based on analytics and statistical methods. *Signa Vitae*, *1*, 15.

Pérez-Arnal, R., Conesa, D., Alvarez-Napagao, S., Suzumura, T., Català, M., Alvarez-Lacalle, E., et al. (2021). Comparative analysis of geolocation information through mobile-devices under different Covid-19 mobility restriction patterns in Spain. *ISPRS International Journal of Geo-Information*, *10*(2), 73.

Pezoa, R., Basso, F., Quilodrán, P., & Varas, M. (2023). Estimation of trip purposes in public transport during the COVID-19 pandemic: The case of Santiago, Chile. *Journal of Transport Geography*, *109*, Article 103594.

Ravindra, K., Goyal, A., & Mor, S. (2021). Does airborne pollen influence COVID-19 outbreak? *Sustainable Cities and Society*, *70*, Article 102887.

Sun, L., Axhausen, K. W., Lee, D.-H., & Huang, X. (2013). Understanding metropolitan patterns of daily encounters. *Proceedings of the National Academy of Sciences*, *110*(34), 13774–13779.

Sun, C., & Zhai, Z. (2020). The efficacy of social distance and ventilation effectiveness in preventing COVID-19 transmission. *Sustainable Cities and Society*, *62*, Article 102390.

Tamblay, S., Galilea, P., Iglesias, P., Raveau, S., & Muñoz, J. C. (2016). A zonal inference model based on observed smart-card transactions for Santiago de Chile. *Transportation Research Part A: Policy and Practice*, *84*, 44–54.

Thomas, N., Jana, A., & Bandyopadhyay, S. (2022). Physical distancing on public transport in Mumbai, India: Policy and planning implications for unlock and post-pandemic period. *Transport Policy*, *116*, 217–236.

Tirachini, A., Hensher, D. A., & Rose, J. M. (2013). Crowding in public transport systems: effects on users, operation and implications for the estimation of demand. *Transportation Research Part A: Policy and Practice*, *53*, 36–52.

Tirachini, A., Hurtubia, R., Dekker, T., & Daziano, R. A. (2017). Estimation of crowding discomfort in public transport: Results from Santiago de Chile. *Transportation Research Part A: Policy and Practice*, *103*, 311–326.

Tiznado, I., Galilea, P., Delgado, F., & Niehaus, M. (2014). Incentive schemes for bus drivers: The case of the public transit system in Santiago, Chile. *Research in Transportation Economics*, *48*, 77–83.

Vuorinen, V., Aarnio, M., Alava, M., Alopaeus, V., Atanasova, N., Auvinen, M., et al. (2020). Modelling aerosol transport and virus exposure with numerical simulations in relation to SARS-CoV-2 transmission by inhalation indoors. *Safety Science*, *130*, Article 104866.

Wang, P., Chen, X., Zheng, Y., Cheng, L., Wang, Y., & Lei, D. (2021). Providing real-time bus crowding information for passengers: A novel policy to promote high-frequency transit performance. *Transportation Research Part A: Policy and Practice*, *148*, 316–329.

Warren, M. S., & Skillman, S. W. (2020). Mobility changes in response to COVID-19. arXiv preprint arXiv:2003.14228.

Wiessing, L., Sypsa, V., Abagiu, A., Arble, A., Berndt, N., Bosch, A., et al. (2022). Impact of COVID-19 & response measures on HIV-HCV prevention services and social determinants in people who inject drugs in 13 sites with recent HIV outbreaks in Europe, North America and Israel. *AIDS and Behavior*, 1–14.

Yap, M., Cats, O., & van Arem, B. (2020). Crowding valuation in urban tram and bus transportation based on smart card data. *Transportmetrica A: Transport Science*, *16*(1), 23–42.

Ying, F., & O'Clery, N. (2021). Modelling COVID-19 transmission in supermarkets using an agent-based model. *PLoS One*, *16*(4), Article e0249821.

Zhang, L., Darzi, A., Ghader, S., Pack, M. L., Xiong, C., Yang, M., et al. (2020). Interactive COVID-19 mobility impact and social distancing analysis platform. *Transportation Research Record*, Article 03611981211043813.

Zhang, Y., Jenelius, E., & Kottenhoff, K. (2017). Impact of real-time crowding information: a Stockholm metro pilot study. *Public Transport*, *9*(3), 483–499.